PROCEEDINGS OF SCIENCE

Status and Developments in Polarised Parton Distribution Functions

Amedeo Chiefa[a,*]

[a]*The Higgs Centre for Theoretical Physics, University of Edinburgh, JCMB, KB, Mayfield Rd, Edinburgh EH9 3JZ, Scotland*

E-mail: amedeo.chiefa@ed.ac.uk

The need for accurate and precise polarised parton distribution functions (PDFs) is becoming increasingly crucial in view of the Electron-Ion Collider experimental program foreseen in the coming years. Two global PDF determinations at next-to-next-to-leading order accuracy have been recently presented, MAPPDFPOL1.0 and BDSSV24. I review the former and I provide a comparative discussion of other PDF sets accurate to next-to-leading order. I show that differences between these PDF sets, due to the choice of experimental and methodological input, exceed differences due to perturbative accuracy.

31st International Workshop on Deep Inelastic Scattering (DIS2024)
8–12 April 2024
Grenoble, France

*Speaker

PoS(DIS2024)200

1. Introduction

Helicity-dependent parton distribution functions (PDFs) [1] are essential for understanding the nucleon spin structure in terms of quarks and gluons [2]. Following the pioneering experiments on polarised deep inelastic scattering (DIS) conducted by the European Muon Collaboration [3, 4], efforts in this field have advanced significantly. The upcoming Electron-Ion Collider (EIC) [5, 6], expected to operate in the 2030s, promises substantial improvements in measuring observables for longitudinally polarised inclusive and semi-inclusive DIS (SIDIS), extending the probed kinematic region (see *e.g.*, Fig. 1 in Ref. [1]) and achieving higher measurement precision.

Future EIC measurements, anticipated to reach the percent-level precision [7], require equally accurate theoretical predictions and PDFs. While there have been several recent advancements in perturbative calculations for both DIS [8–15] and SIDIS [16–18] structure functions, the bulk of the available polarised PDF sets remains, to date, at next-to-leading order (NLO) [19–21].

Very recently, two new NNLO analyses of polarised PDFs have been presented in Refs. [22, 23], although only the PDF sets in Ref. [23] have been made public. Both determinations are based on available DIS and SIDIS data, but Ref. [22] also includes proton-proton (pp) spin asymmetry data from the Relativistic Heavy Ion Collider (RHIC). These determinations extend a previous NNLO analysis based on solely DIS data [24], and will be followed by a new NNLO determination [25]. Here, I briefly discuss MAPPDFPOL1.0, the new polarised PDF set presented in Ref. [23], before moving to a comparative analysis of the currently available polarised PDF sets at NLO.

2. MAPPDFpol1.0 at NNLO

The polarised PDF set MAPPDFPOL1.0 presented in Ref. [23] leverages a fitting framework that combines a neural-network parametrisation [26] of polarised PDFs with a Monte Carlo representation of PDF uncertainties, aiming at reducing parametrisation bias as much as possible and at obtaining statistically sound uncertainties.

The experimental information included in MAPPDFPOL1.0 relies on the currently available structure function data for inclusive [4, 27–37] and semi-inclusive [38, 39] DIS. In addition, SU(2) and SU(3) flavour symmetries are assumed to hold exactly, so that the lowest moments of the triplet and octet polarised PDF combinations can be compared to the values extracted from semi-leptonic β-decays [40]. The parametrised flavours are Δf_u, $\Delta f_{\bar{u}}$, Δf_d, $\Delta f_{\bar{d}}$, Δf_s, $\Delta f_{\bar{s}}$, and Δf_g. The initial parametrisation scale is $Q^2 = 1$ GeV^2. Note that Δf_s and $\Delta f_{\bar{s}}$ are parametrised separately thanks to the charged kaon production in SIDIS data and to the NNLO corrections which make strange quark and antiquark evolve differently. Finally, the positivity constraint of cross-sections is enforced through the PDFs by imposing $|\Delta f| \leq f$.

Theoretical predictions are computed using the public code APFEL++ [41, 42]. Polarised coefficient functions for DIS are implemented using exact calculations up to NNLO [43], and massive-quark corrections for g_1 are omitted. SIDIS coefficient functions are implemented up to NLO [44, 45], while NNLO corrections are included via the approximate threshold resummation formalism [16]. The recent exact polarised coefficient functions for SIDIS computed in Refs. [17, 18] are not yet implemented in MAPPDFpol1.0 nor in Ref. [22]. Intrinsic heavy-quark distributions are considered to be identically zero below their respective thresholds. Above these

thresholds, heavy-quark distributions are perturbatively generated by means of DGLAP evolution in the zero-mass variable-flavour-number scheme (ZM-VFNS). Perturbative corrections to the splitting functions in the DGLAP equations are consistently included up to NNLO accuracy [46–48].

At NNLO, the resulting up- and down-quark polarised distributions are well constrained by data, although sea-quark and gluon distributions remain largely uncertain and compatible with zero. Despite the inclusion of SIDIS data and NNLO corrections, the polarised strange asymmetry remains compatible with zero. NNLO corrections lead to a slight deterioration of the global fit quality, especially with SIDIS data. Overall, the impact of NNLO corrections on distributions is moderate, as also confirmed in Ref. [22]. Theoretical constraints on SU(2) and SU(3) flavour symmetries have minimal effects, but the positivity constraint significantly affects the shape and uncertainty of PDFs in the large-x region.

This analysis can be improved on different fronts, starting from the implementation of the exact SIDIS computations. Indeed, although the terms common to the threshold-expanded and the complete computation are in excellent agreement between them, the gluon-gluon channels that open at NNLO in the exact calculations may affect the polarised gluon. Furthermore, NNLO calculations introduce significant corrections to the approximate computation in the region $x \lesssim 0.1$, which may be one of the possible causes for the deterioration of the fit quality when moving to NNLO. Indeed, the same deterioration is not observed in Ref. [22], where a cut $x > 0.12$ is applied to SIDIS data. Thus, the implementation of the exact calculations is left for future work.

3. The current status of polarised PDFs at NLO

Although NNLO accuracy is going to be the new standard for future determinations of polarised PDFs, the majority of the current available information remains at NLO. Despite the limited accuracy of NLO analyses, a comparative study of polarised PDF sets at this level can provide valuable insights resulting from the choices made in the data sets and in the methodological approaches. Furthermore, NLO determinations implement exact DIS and, where present, SIDIS calculations for the structure functions, thereby minimising the dependence on potential errors associated with approximate perturbative calculations.

Some of the most recent and most widely used sets of polarised PDFs at NLO accuracy are MAPPDFPOL1.0 [23], NNPDFpol1.1 [20], JAM17 [21], and DSSV14 [49][1]. In the following, I provide a brief description for each set listed above.

- **NNPDFpol1.1** This set includes open-charm production in fixed-target DIS, and jet and W production in proton-proton collisions at RHIC, in addition to inclusive DIS data. Target mass corrections are also included for the structure function g_1. The positivity constraint is applied to polarised PDFs, and sum rules are used to impose SU(2) and SU(3) flavour symmetries. PDFs are parametrised with a neural network and uncertainties are estimated using the Monte Carlo replica method.

- **DSSV14** In addition to inclusive and semi-inclusive DIS data, this set takes into account data for jet and hadron production in proton-proton collisions at RHIC. A fixed functional form

[1] The list should also include BDSSV22, the NLO polarised PDF set presented in Ref. [22]. However, together with the NNLO determination BDSSV24, these sets are not publicly available.

is used to parametrise the PDFs and, in the Monte Carlo variant of DSSV14 [49], uncertainties are estimated using Monte Carlo sampling. The positivity constraint is also enforced to distributions, and two parameters are used to account for deviations from the assumption of SU(2) and SU(3) flavour symmetries.

- **JAM17** This set includes data for inclusive and semi-inclusive DIS, together with single-inclusive e^+e^- annihilation (SIA) data. This set is obtained by performing a simultaneous fit of both PDFs and fragmentation functions, both parametrised in terms of a fixed function normalised to Euler beta functions. This set does not include positivity nor assumptions about SU(2) and SU(3) flavour symmetries. Also in this case, uncertainties have been estimated by means of Monte Carlo sampling.

The aforementioned sets are compared in Fig. 1, which shows Δf_u, $\Delta f_{\bar{u}}$, Δf_d, $\Delta f_{\bar{d}}$, Δf_s, $\Delta f_{\bar{s}}$, Δf_c, and Δf_g as functions of x at the scale $Q^2 = 10\ \text{GeV}^2$. For all PDF sets, error bands correspond to the one-sigma uncertainty.

The inclusion of gluon-sensitive data helps pin down the polarised gluon PDF, as it can be seen for NNPDFpol1.1 and DSSV14. RHIC pp data has significant effects in the region $x \gtrsim 10^{-3}$, leaving the range $10^{-3} \lesssim x \lesssim 10^{-2}$ less constrained [49]. These features are qualitatively consistent between NNPDFpol1.1 and DSSV14. Open-charm production data, included in NNPDFpol1.1, has been shown [20] to have negligible effects on the polarised gluon PDF. The absence of gluon-initiated data in MAPPDFPOL1.0 is noticeable in the mid-x region (covered by RHIC data), where uncertainties are larger. On the other hand, JAM17, albeit having an array of data similar to MAPPDFPOL1.0, has smaller uncertainty bands, which may suggest a potential bias in the parametrisation. Nevertheless, all distributions are compatible within uncertainties.

The up- and down-quark distributions are generally in good agreement amongst the different PDF sets. In the low-x region, where DIS and SIDIS data is sparse, MAPPDFPOL1.0 provides more conservative uncertainties. Deviations are more noticeable in the case of up- and down-antiquark distributions. In the region $x \gtrsim 5 \times 10^{-1}$, the $\Delta f_{\bar{u}}$ PDF from MAPPDFPOL1.0 is pulled closer to DSSV14, which also includes SIDIS data, and away from NNPDFpol1.1, which does not. This feature was already noted in Ref. [20], where it was observed that the STAR W asymmetry pulled $\Delta f_{\bar{u}}$ in a different direction than the SIDIS data used in MAPPDFPOL1.0 and DSSV14.

In the case of the strange PDFs, the compared sets present different behaviours. Note that only MAPPDFPOL1.0 allows Δf_s to be different from $\Delta f_{\bar{s}}$, and JAM17 parametrises $\Delta f_{\bar{s}}$ and Δf_s^+. DSSV14 sets $\Delta f_s = \Delta f_{\bar{s}}$, while NNPDFpol1.1 fits Δf_s^+. In MAPPDFPOL1.0, JAM17, and DSSV14 the Δf_s^+ PDF is mainly driven by SIDIS data, while the NNPDFpol1.1 constraining power derives from the inclusion of the semi-leptonic β-decay parameters. The effect of the different data sets can be seen in the central-x region, where deviations between NNPDFpol1.1 and DSSV14 are not contained in the relative uncertainties. MAPPDFPOL1.0 delivers more conservative uncertainties, and the shape of Δf_s and $\Delta f_{\bar{s}}^+$ is more consistent with that given by the DSSV group. The PDFs from JAM17, on the other hand, are those that provide the least conservative uncertainties despite using a similar experimental information as MAPPDFPOL1.0.

Finally, intrinsic polarised Δc is not parametrised in any of the compared sets. In MAPPDFPOL1.0, NNPDFpol1.1, and JAM17, polarised Δc is generated by gluon splitting in the perturbative

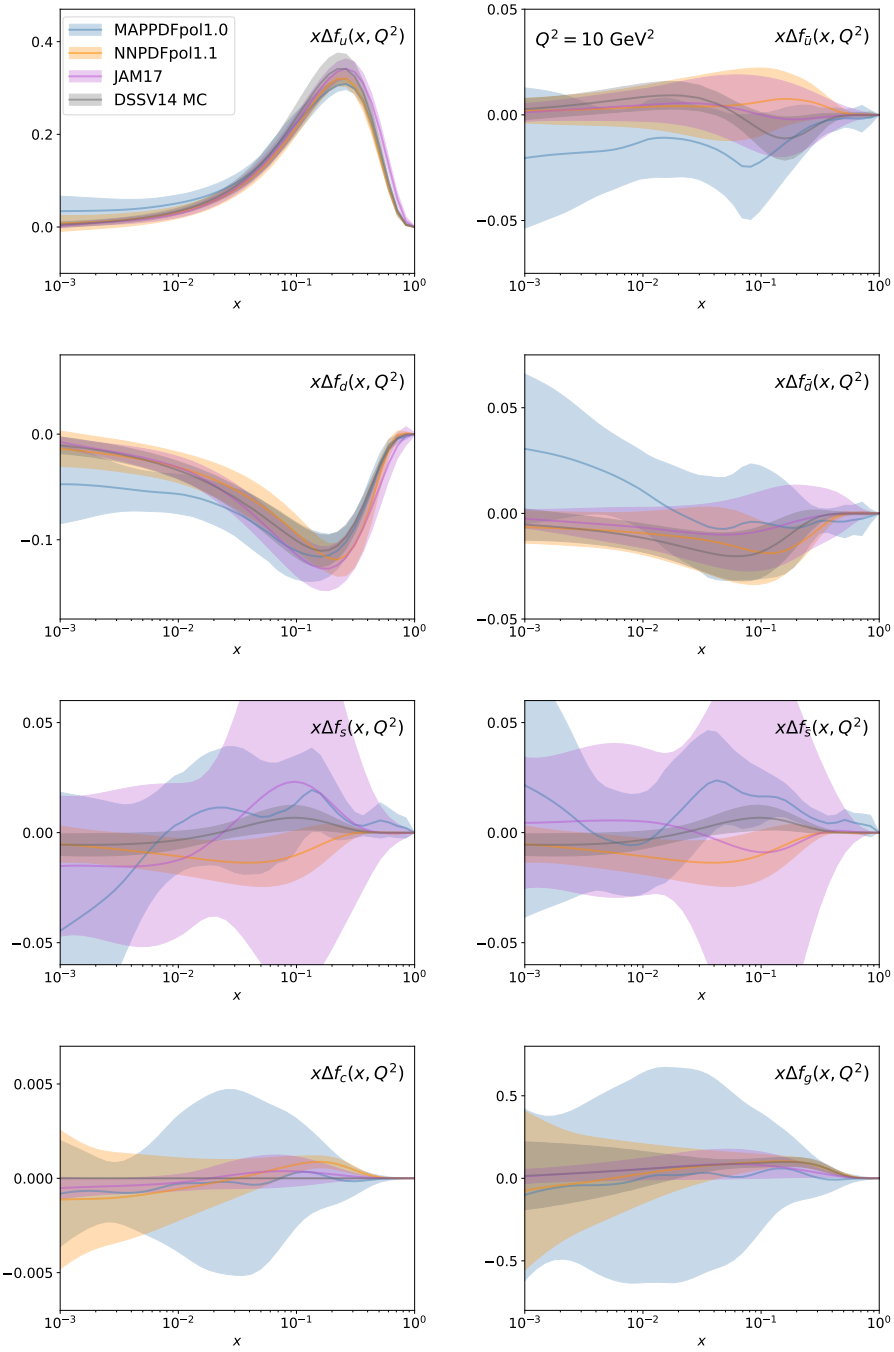

Figure 1: Comparison of the MAPPDFPOL1.0, NNPDFpol1.1 [20], JAM17 [21], and DSSV14 [49] polarised PDF sets at NLO. Distributions are shown as functions of x at $Q^2 = 10$ GeV^2. Error bands correspond to one-sigma uncertainties.

evolution, and indeed they show similar behaviour as Δg. Note that the polarised charm PDF in the DSSV14 Monte Carlo grid has been set to zero.

4. Conclusions

The comparative analysis conducted at NLO shows that experimental input and methodological approach significantly influence the resulting polarised PDFs. Conversely, the analyses of MAPPDFPOL1.0 and BDSSV24 show that the differences between the respective NLO and NNLO sets are moderate and smaller than those observed at fixed perturbative order in Fig. 1. This suggests that a similar trend to that shown in Fig. 1 is likely to be observed across multiple polarised PDF sets when an analogous comparative analysis will be undertaken at NNLO level. Therefore, benchmarking across different PDF sets would be essential to identify the potential sources of the observed differences, whether they stem from the methodological or experimental input.

References

[1] J.J. Ethier and E.R. Nocera, *Parton Distributions in Nucleons and Nuclei*, *Ann. Rev. Nucl. Part. Sci.* **70** (2020) 43 [2001.07722].

[2] X. Ji, F. Yuan and Y. Zhao, *What we know and what we don't know about the proton spin after 30 years*, *Nature Rev. Phys.* **3** (2021) 27 [2009.01291].

[3] EUROPEAN MUON collaboration, *A Measurement of the Spin Asymmetry and Determination of the Structure Function g(1) in Deep Inelastic Muon-Proton Scattering*, *Phys. Lett. B* **206** (1988) 364.

[4] EUROPEAN MUON collaboration, *An Investigation of the Spin Structure of the Proton in Deep Inelastic Scattering of Polarized Muons on Polarized Protons*, *Nucl. Phys. B* **328** (1989) 1.

[5] R. Abdul Khalek et al., *Science Requirements and Detector Concepts for the Electron-Ion Collider: EIC Yellow Report*, *Nucl. Phys. A* **1026** (2022) 122447 [2103.05419].

[6] R. Abdul Khalek et al., *Snowmass 2021 White Paper: Electron Ion Collider for High Energy Physics*, 2203.13199.

[7] I. Borsa, G. Lucero, R. Sassot, E.C. Aschenauer and A.S. Nunes, *Revisiting helicity parton distributions at a future electron-ion collider*, *Phys. Rev. D* **102** (2020) 094018 [2007.08300].

[8] J. Blümlein, P. Marquard, C. Schneider and K. Schönwald, *The massless three-loop Wilson coefficients for the deep-inelastic structure functions F_2, F_L, xF_3 and g_1*, *JHEP* **11** (2022) 156 [2208.14325].

[9] F. Hekhorn and M. Stratmann, *Next-to-Leading Order QCD Corrections to Inclusive Heavy-Flavor Production in Polarized Deep-Inelastic Scattering*, *Phys. Rev. D* **98** (2018) 014018 [1805.09026].

[10] A. Behring, J. Blümlein, A. De Freitas, A. von Manteuffel and C. Schneider, *The 3-Loop Non-Singlet Heavy Flavor Contributions to the Structure Function $g_1(x, Q^2)$ at Large Momentum Transfer*, *Nucl. Phys. B* **897** (2015) 612 [1504.08217].

[11] J. Ablinger, A. Behring, J. Blümlein, A. De Freitas, A. von Manteuffel, C. Schneider et al., *The three-loop single mass polarized pure singlet operator matrix element*, *Nucl. Phys. B* **953** (2020) 114945 [1912.02536].

[12] A. Behring, J. Blümlein, A. De Freitas, A. von Manteuffel, K. Schönwald and C. Schneider, *The polarized transition matrix element $A_{gq}(N)$ of the variable flavor number scheme at $O(\alpha_s^3)$*, *Nucl. Phys. B* **964** (2021) 115331 [2101.05733].

[13] J. Blümlein, A. De Freitas, M. Saragnese, C. Schneider and K. Schönwald, *Logarithmic contributions to the polarized O(αs3) asymptotic massive Wilson coefficients and operator matrix elements in deeply inelastic scattering*, *Phys. Rev. D* **104** (2021) 034030 [2105.09572].

[14] I. Bierenbaum, J. Blümlein, A. De Freitas, A. Goedicke, S. Klein and K. Schönwald, *$O(\alpha_s^2)$ polarized heavy flavor corrections to deep-inelastic scattering at $Q^2 \gg m^2$*, *Nucl. Phys. B* **988** (2023) 116114 [2211.15337].

[15] J. Ablinger, A. Behring, J. Blümlein, A. De Freitas, A. von Manteuffel, C. Schneider et al., *The first-order factorizable contributions to the three-loop massive operator matrix elements $A_{Qg}^{(3)}$ and $\Delta A_{Qg}^{(3)}$*, 2311.00644.

[16] M. Abele, D. de Florian and W. Vogelsang, *Approximate NNLO QCD corrections to semi-inclusive DIS*, *Phys. Rev. D* **104** (2021) 094046 [2109.00847].

[17] L. Bonino, T. Gehrmann, M. Löchner, K. Schönwald and G. Stagnitto, *Polarized semi-inclusive deep-inelastic scattering at NNLO in QCD*, 2404.08597.

[18] S. Goyal, R.N. Lee, S.-O. Moch, V. Pathak, N. Rana and V. Ravindran, *NNLO QCD corrections to polarized semi-inclusive DIS*, 2404.09959.

[19] D. de Florian, R. Sassot, M. Stratmann and W. Vogelsang, *Evidence for polarization of gluons in the proton*, *Phys. Rev. Lett.* **113** (2014) 012001 [1404.4293].

[20] NNPDF collaboration, *A first unbiased global determination of polarized PDFs and their uncertainties*, *Nucl. Phys. B* **887** (2014) 276 [1406.5539].

[21] J.J. Ethier, N. Sato and W. Melnitchouk, *First simultaneous extraction of spin-dependent parton distributions and fragmentation functions from a global QCD analysis*, *Phys. Rev. Lett.* **119** (2017) 132001 [1705.05889].

[22] I. Borsa, D. de Florian, R. Sassot, M. Stratmann and W. Vogelsang, *NNLO Global Analysis of Polarized Parton Distribution Functions*, 2407.11635.

[23] MAP collaboration, *Helicity-dependent parton distribution functions at next-to-next-to-leading order accuracy from inclusive and semi-inclusive deep-inelastic scattering data*, 2404.04712.

[24] F. Taghavi-Shahri, H. Khanpour, S. Atashbar Tehrani and Z. Alizadeh Yazdi, *Next-to-next-to-leading order QCD analysis of spin-dependent parton distribution functions and their uncertainties: Jacobi polynomials approach*, *Phys. Rev. D* **93** (2016) 114024 [1603.03157].

[25] F. Hekhorn, *Towards NNPDFpol2.0*, in *31st International Workshop on Deep-Inelastic Scattering and Related Subjects*, 6, 2024 [2406.06083].

[26] R. Abdul Khalek and V. Bertone, *On the derivatives of feed-forward neural networks*, 2005.07039.

[27] Spin Muon collaboration, *Spin asymmetries A(1) and structure functions g1 of the proton and the deuteron from polarized high-energy muon scattering*, *Phys. Rev. D* **58** (1998) 112001.

[28] COMPASS collaboration, *The spin structure function g_1^p of the proton and a test of the Bjorken sum rule*, *Phys. Lett. B* **753** (2016) 18 [1503.08935].

[29] COMPASS collaboration, *Final COMPASS results on the deuteron spin-dependent structure function g_1^d and the Bjorken sum rule*, *Phys. Lett. B* **769** (2017) 34 [1612.00620].

[30] E142 collaboration, *Deep inelastic scattering of polarized electrons by polarized He-3 and the study of the neutron spin structure*, *Phys. Rev. D* **54** (1996) 6620 [hep-ex/9610007].

[31] E143 collaboration, *Measurements of the proton and deuteron spin structure functions g(1) and g(2)*, *Phys. Rev. D* **58** (1998) 112003 [hep-ph/9802357].

[32] E154 collaboration, *Precision determination of the neutron spin structure function g1(n)*, *Phys. Rev. Lett.* **79** (1997) 26 [hep-ex/9705012].

[33] E155 collaboration, *Measurements of the Q**2 dependence of the proton and neutron spin structure functions g(1)**p and g(1)**n*, *Phys. Lett. B* **493** (2000) 19 [hep-ph/0007248].

[34] HERMES collaboration, *Measurement of the neutron spin structure function g1(n) with a polarized He-3 internal target*, *Phys. Lett. B* **404** (1997) 383 [hep-ex/9703005].

[35] HERMES collaboration, *Precise determination of the spin structure function g(1) of the proton, deuteron and neutron*, *Phys. Rev. D* **75** (2007) 012007 [hep-ex/0609039].

[36] Jefferson Lab Hall A collaboration, *Measurements of d_2^n and A_1^n: Probing the neutron spin structure*, *Phys. Rev. D* **94** (2016) 052003 [1603.03612].

[37] CLAS collaboration, *Precision measurements of g_1 of the proton and the deuteron with 6 GeV electrons*, *Phys. Rev. C* **90** (2014) 025212 [1404.6231].

[38] COMPASS collaboration, *Quark helicity distributions from longitudinal spin asymmetries in muon-proton and muon-deuteron scattering*, *Phys. Lett. B* **693** (2010) 227 [1007.4061].

[39] HERMES collaboration, *Longitudinal double-spin asymmetries in semi-inclusive deep-inelastic scattering of electrons and positrons by protons and deuterons*, *Phys. Rev. D* **99** (2019) 112001 [1810.07054].

[40] Particle Data Group collaboration, *Review of Particle Physics*, *PTEP* **2022** (2022) 083C01.

[41] V. Bertone, S. Carrazza and J. Rojo, *APFEL: A PDF Evolution Library with QED corrections*, *Comput. Phys. Commun.* **185** (2014) 1647 [1310.1394].

[42] V. Bertone, *APFEL++: A new PDF evolution library in C++*, *PoS* **DIS2017** (2018) 201 [1708.00911].

[43] E.B. Zijlstra and W.L. van Neerven, *Order-α_s^2 corrections to the polarized structure function $g_1(x, Q^2)$*, *Nucl. Phys. B* **417** (1994) 61.

[44] W. Furmanski and R. Petronzio, *Lepton - Hadron Processes Beyond Leading Order in Quantum Chromodynamics*, *Z. Phys. C* **11** (1982) 293.

[45] D. de Florian, M. Stratmann and W. Vogelsang, *QCD analysis of unpolarized and polarized Lambda baryon production in leading and next-to-leading order*, *Phys. Rev. D* **57** (1998) 5811 [hep-ph/9711387].

[46] S. Moch, J.A.M. Vermaseren and A. Vogt, *The Three-Loop Splitting Functions in QCD: The Helicity-Dependent Case*, *Nucl. Phys. B* **889** (2014) 351 [1409.5131].

[47] S. Moch, J.A.M. Vermaseren and A. Vogt, *On $\gamma 5$ in higher-order QCD calculations and the NNLO evolution of the polarized valence distribution*, *Phys. Lett. B* **748** (2015) 432 [1506.04517].

[48] J. Blümlein, P. Marquard, C. Schneider and K. Schönwald, *The three-loop polarized singlet anomalous dimensions from off-shell operator matrix elements*, *JHEP* **01** (2022) 193 [2111.12401].

[49] D. De Florian, G.A. Lucero, R. Sassot, M. Stratmann and W. Vogelsang, *Monte Carlo sampling variant of the DSSV14 set of helicity parton densities*, *Phys. Rev. D* **100** (2019) 114027 [1902.10548].